Interface shape dependent interference patterns of NbSe2 heterostructure Josephson junctions

Chen, X.; Poortvliet, M.T.L.; Molen, S.J. van der; Dood, M.J.A. de

Interface shape dependent interference patterns of $NbSe_2$ heterostructure Josephson junctions

Xingchen Chen,* Mio Poortvliet,* Sense Jan van der Molen, and Michiel J. A. de Dood
Huygens-Kamerlingh Onnes Laboratory, Leiden University, P.O. Box 9504, 2300 RA Leiden, The Netherlands

(Received 28 December 2022; accepted 21 March 2023; published 31 March 2023)

The superconducting critical current oscillations as a function of magnetic field were previously observed in heterostructure Josephson junctions fabricated by twisting and stacking superconducting van der Waals materials. The interference patterns, however, are often distorted. Here, we report a model for understanding the shape of oscillation patterns in heterostructure Josephson junctions. To this end, we fabricated Josephson junctions by stacking two bulk superconducting $2H$-$NbSe_2$ flakes on top of each other. We were able to control the junction fabricated to be either diffusive or clean by varying the temperature during the stacking process. The measured magnetic field dependence of the critical current exhibits either a Gaussian decay or a clear oscillatory pattern with maxima and minima. We identify the shape of the interference patterns not only depends on the type of junction; they are also strongly dictated by field orientation and interface geometry. This is a consequences of the fact that heterostructure junctions often have inhomogeneous widths that extend along the field direction. We calculate the expected interference pattern from the junction geometry by applying our model and find excellent agreement to our experimental data.

DOI: 10.1103/PhysRevB.107.094522

I. INTRODUCTION

Van der Waals materials refer to highly anisotropic layered materials that possess strong chemical bonds in the in-plane direction, while the layers are kept together by the van der Waals force. The most famous example is graphene, which was first successfully isolated in 2004 from graphite [1]. Since then, the family of van der Waals materials has provided a new playground for studying and understanding quantum phenomena [2,3].

Recent research shows that by stacking and twisting the same or different van der Waals materials vertically into a heterostructure, the properties (including the band structure) of such systems change with respect to its pristine materials [4–7]. This adds another degree of freedom in tuning such materials' properties.

Utilizing the recent development in the cleaving and micromanipulating technique [8–11], van der Waals materials provide a platform for fabricating Josephson junctions innovatively by making heterostructures. Interestingly, the weak link needed for a Josephson junction can be produced by stacking two flakes on top of each other, at nonzero twist angle [12,13]. Alternatively, it is also possible to introduce a different material in between the superconductor to act as a weak link [14,15].

Previous work has shown that it is possible to construct a highly transparent van der Waals Josephson junction by decoupling and recoupling two bulk $2H$-$NbSe_2$ flakes [16]. It was later reported that the supercurrent density strongly depends on the twist angles between the two flakes which also correlates to whether the junction is overdamped or underdamped [17]. It was shown that underdamped junctions provide a gateway for building superconducting diode devices with such heterostructures [15]. A superconducting quantum interference device (SQUID) was also demonstrated by etching one single junction device [17]. However, the reported junctions' critical current dependency on an external magnetic field is often distorted from the usually seen Fraunhofer pattern. A closer consideration on such irregularity is yet to be realized.

Here, we report a model for understanding the superconducting critical current oscillation behavior under an external magnetic field for heterostructure Josephson junctions. To test it, we constructed Josephson junctions by stacking two superconducting $NbSe_2$ flakes together. We can obtain either diffusive or clean junctions by varying the flake temperature during our junctions' fabrication processes. For our diffusive junctions, a Gaussian shape is found, as expected. For our clean junctions an anomalous critical current oscillation patterns under an in-plane magnetic field is observed, comparable to what has been reported elsewhere.

By applying our model (based on Ref. [18]) to a clean junction we show that it is possible to recover the irregular interference pattern from the junctions' geometry. Moreover, we show the interference patterns have a strong field orientation dependency. At some field angles a clean junction can even exhibit a Gaussian-like critical current decay. We believe this is why the "ideal" Fraunhofer pattern is not often measured in heterostructure junctions.

We also find and address a discrepancy in the calculated c-axis penetration depth, and propose possible reasons. Interestingly, this discrepancy happens between the penetration depth calculated by junction transport measurements and the penetration depth measured by other methods. The penetration depth observed from our work is consistent with those

*These authors contributed equally to this work.

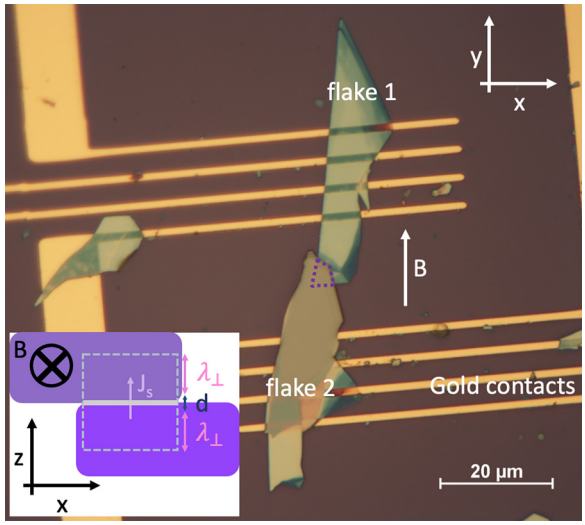

FIG. 1. Optical microscope image for a typical device with two bulk $NbSe_2$ flakes. The junction region is highlighted by purple dashed lines. The two flakes lie in the x-y plane, while the current flow in the z direction crosses the junction. An in-plane magnetic field is applied. The inset shows a schematic cross section of the two flakes (x-z plane). The interface of the flakes is marked with the gray line whereas the weak link of the junction is marked by the gray dashed rectangle.

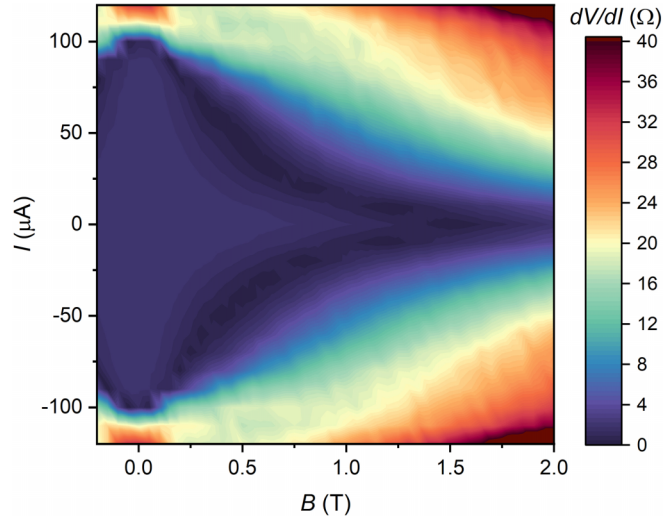

FIG. 2. A false color plot of differential resistance dV/dI as a function of an in-plane magnetic field and applied current measured at 2.0 K. Data were obtained by taking the $I(V)$ curves while sweeping the magnetic field from the negative to the positive direction.

stated from previous transport works [15–17] on similar junctions.

II. METHODS

A standard lithography process was used to write gold contacts on a bare SiO(300 nm)/Si substrate. With the help of a commercially available stamping stage (HQ graphene), the two flakes are stamped, with a small overlapping region, on top of the gold contacts. The stamping process follows the standard dry transfer method using only polydimethylsiloxane (PDMS) polymer film as a pick-up and drop-down stamp [19]. The fabrication was conducted in ambient conditions. However, because $NbSe_2$ is highly sensitive to oxidation, the device-to-air contact time was limited to 1 h [16].

The individual flake's thickness is selected to be between 20 and 90 nm. This ensures that the two parts of the junction have the same superconducting transition temperature. Flakes thinner than 10 nm could have a critical temperature below 7 K [3] and would therefore decrease device quality.

An optical microscope image of a typical device is shown in Fig. 1. The gold contacts are below the flakes and the overlapping region of the two flakes is the junction interface (highlighted with the purple dashed line). The bias current flows vertically across the interface, in the direction normal to the substrate plane. The magnetic field is in the in-plane direction, making it normal to the supercurrent.

The cross section of the device is illustrated in the inset in Fig. 1. The interface of the two flakes is highlighted by the gray line, and has a thickness of d. The dashed light gray rectangle represents the junction weak link, which extends a distance equal to the c-axis penetration depth ($\lambda_\perp$) into both flakes.

Some degree of oxidation at the interface is always to be expected. The nature of the junction depends on how heavy the oxidation is at the interface between two flakes. By varying the temperature during the stamping process, we can exert some control over weather the fabricated junction is in the clean or diffusive limit.

III. RESULTS

A. Diffusive junctions

We first show we are able to fabricate both diffusive junctions and clean junctions. Device 1 is obtained by heating the flakes to a temperature of 180 °C in ambient conditions during stamping the flakes to the contacts.

Because the heating element promotes oxidation, we expect a disordered layer to cover most of the interface of the two bulk superconducting electrodes. This disordered layer pushes the junction to the dirty limit where the mean free path for the electron is much smaller than the junction length. As a result, the junction moves towards the diffusive limit.

Under a magnetic field perpendicular to the junction's supercurrent, theory predicts a Gaussian decays of the critical current as a function of the field strength. In Fig. 2, we present the differential resistance dV/dI as a function of an in-plane magnetic field strength and the applied current for a heavily oxidized device that is expected to be in the diffusive limit (device 1).

The junction's critical current decays quickly following a Gaussian curve peak at zero field. There is no oscillation in the critical current decay (also not at higher fields; not shown), showing a clear diffusive junction Gaussian decay curve.

B. Clean junctions

When no heating was applied during the device fabrication, clear oscillation patterns are observed in the measured critical current as a function of in-plane magnetic field. Figure 3

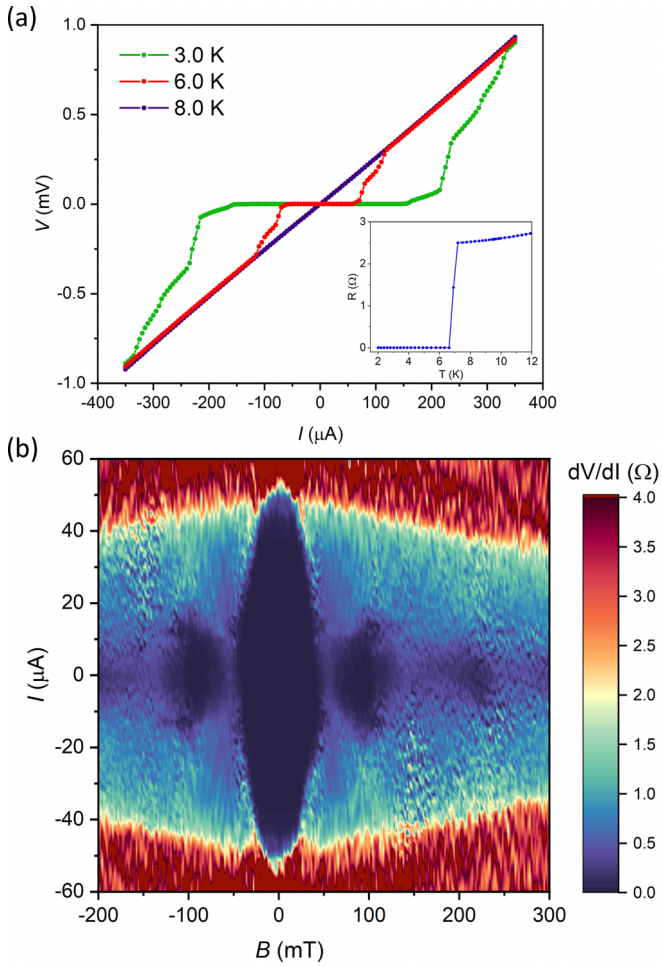

FIG. 3. (a) $I(V)$ curves at different temperatures showing multiple steplike transitions below T_c. However, there is no clear transition that separates the bulk superconductor and the junction in resistance as a function of temperature (see inset). (b) False color plot of dV/dI as a function of the in-plane magnetic field and applied current at $T = 6.5$ K. The critical current dependency shows clear Fraunhofer-like oscillations, though distorted.

shows results for device 2. The junction has a critical temperature of 7.0 K, shown in the inset of Fig. 3(a). The individual transitions of the junction and the rest of the bulk flakes can be clearly seen in the $I(V)$ curves in Fig. 3(a), where the data showing multiple steps before the normal state resistance is reached. This signifies the critical current for the junction is smaller than the critical current for both bulk superconductor.

The junction has little to no hysteresis behavior, suggesting there is no significant retrapping current and the junction is overdamped. This indicates that the weak link has a very small capacitance effect on the junction. The high critical current density (620 kA/cm^2 at 3.0 K) indicates the interface is highly transparent. The overdamped high transparent junction well supports the assumption that the weak link comes from twisting and stacking instead of oxidation or a dirt layer in between the two flakes.

For a planar junction, a Fraunhofer pattern is typically observed for the measured critical current as a function of magnetic field strength. However, in our junction, the observed pattern shape [see Fig. 3(b)] is less well developed and misses most sidelobes. The size of the sidelobes also changes very rapidly with the magnetic field. An anomalous interference pattern in a magnetic field is observed in many of our devices.

In the Analysis section, we argue this is not a trivial effect caused by device qualities or measurement artifacts. It is instead caused by the fact that the junction has irregular widths along the magnetic field direction.

IV. ANALYSIS AND DISCUSSION

The way to calculate supercurrent distribution and a critical current magnetic interference pattern in Josephson junctions was thoroughly discussed in Ref. [18]. Here, we want to focus on a stacked heterostructure junction geometry, assuming the current density is homogeneous everywhere across the junction and solely in the z direction. The light dashed gray rectangle in the schematic illustration in Fig. 1 demonstrates where the flux loop of the junction is drawn. For each x-z cross section, the magnetic flux $\Phi = AB = (2\lambda_\perp + d)XB$, where $\lambda_\perp$ is the c-axis penetration depth, d is the thickness of the interface, and X is the junction width. Given the size of d being much smaller than $\lambda_\perp$ in clean stacking junctions, we consider d to be negligible. We fix the in-plane magnetic field direction to be in the y direction. The specific directions in real experiments are not lost as the frame of reference can always be rotated to allow the B field to be fixed to the y direction.

For one slice of the junction of width dy in the y direction, the current can be described as [18]

$$I_x(B) = \mathrm{Im}\left[e^{-i\phi_0}\int_{-\infty}^{\infty} J_s e^{i\beta x}\,dx\right], \tag{1}$$

where ϕ_0 is the phase factor of the supercurrent, $\beta = 4\pi B\lambda_\perp/\Phi_0$, and J_s is the two-dimensional (2D) supercurrent density in units of A/m. Because we are only interested in the critical current, where $I(B)$ is largest, the value for phase factor ϕ_0 can be dropped from the equation. In other words, the critical current of this slice scales with the Fourier transform of the current density in the direction perpendicular to the magnetic field. This equation describes the critical current behavior of every x-z slice throughout the interface. Because the junction also extends along the magnetic field direction, the complete critical current calculation is the sum of all the slices in the y direction. Hence, the total critical current in a magnetic field is described by

$$I_c(B) = \left|\int_{-\infty}^{\infty}\int_{-\infty}^{\infty} J_s e^{i\beta x}\,dx\,dy\right|. \tag{2}$$

In practice, these integrals will run over the irregular area defined by the overlap of the two flakes, generating the specific critical current pattern given a known field direction.

Figure 4 shows the results of the method given by Eq. (2) applied to device 2 for every field orientation. The interface area was determined by the microscope image of the device. We assume the whole overlapping region to be the junction area, and the current density to be homogeneous everywhere across the junction. Figure 4 shows that the dependency of critical current on the magnetic fields varies considerably with the field direction. The central peak is pronounced

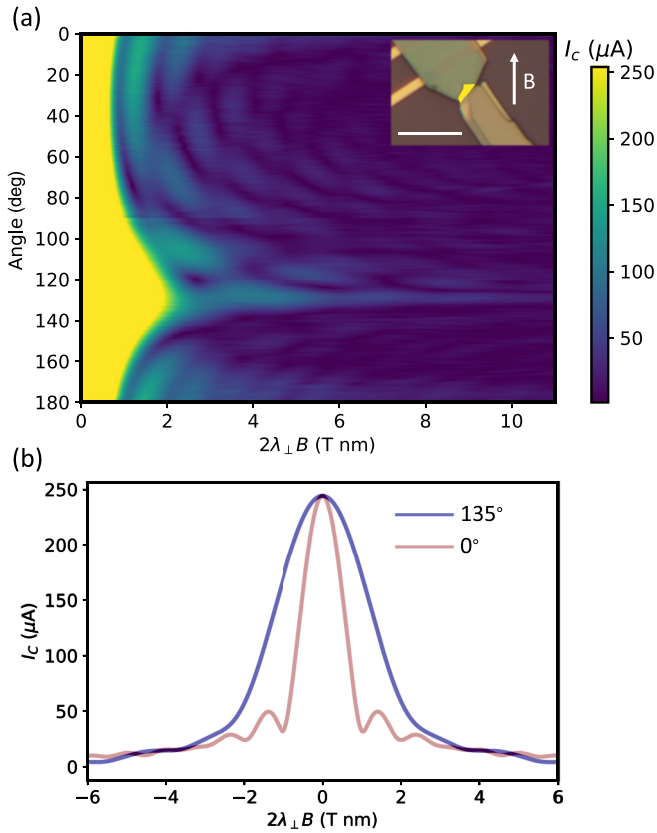

FIG. 4. (a) False color plot of calculated critical current as a function of magnetic field strength and orientation, where the inset shows the microscope image of the device at 0° orientation, and the scale bar represents 10 μm. (b) Comparison of the interference pattern between 0° and 135°, showing the interference pattern of the same device has a strong dependence on field orientation.

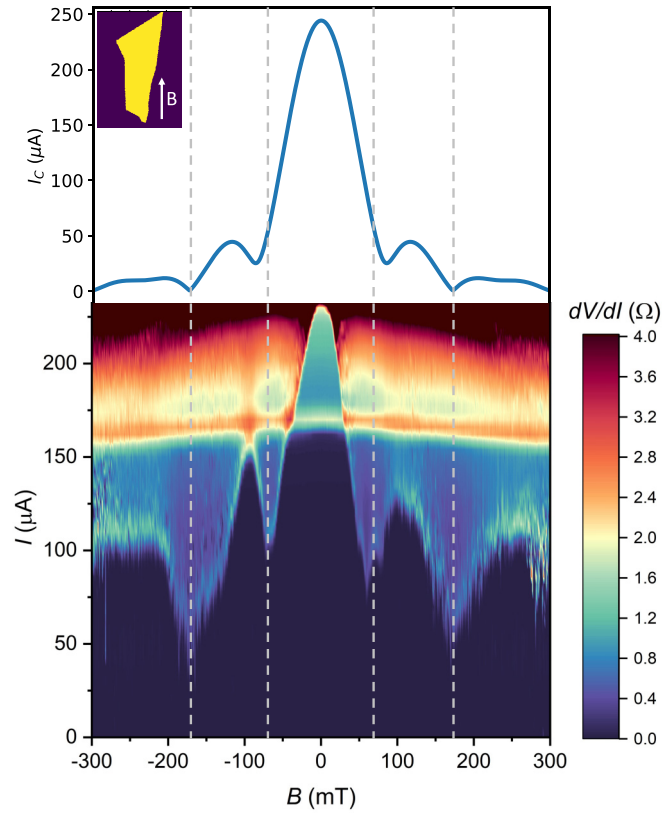

FIG. 5. The calculated critical current as a function of magnetic field strength at 35° compared to the measured Fraunhofer pattern on the device at 1.5 K, where the junction area field orientation is shown in the inset of the upper panel.

at all orientations and the distortion in both the amplitude and span of the sidelobes for most of the field directions is evident.

It is interesting that a Gaussian-like decay is also observed at some angles, e.g., around 130°–150°, which is not expected for a clean junction. See Fig. 4(b) for a comparison between 0° orientation and 135°. Along with a strong suppression of sidelobes in almost all field directions, this may explain why it is relatively difficult to measure oscillation patterns in heterostructure junctions.

We now present results of a more exact comparison between our calculations and our measurements. The oscillation pattern obtained from device 2 was measured under a field orientation of approximately 35°, and the geometry is shown in the upper panel inset in Fig. 5. The calculated critical current as a function of magnetic field strength at 35° is plotted in the upper panel of Fig. 5, and for the lower panel we show our experimentally obtained pattern at 1.5 K. The two patterns have strikingly similar shapes. As shown by the dashed gray line, the minima and peak shape of the interference pattern correspond very well with the calculation of our model. We believe we have thus interpreted the irregularity in the observed critical current oscillation pattern as the Josephson effect under magnetic flux in a junction with an irregular shape.

In order to get good quantitative agreement, we have had to plug in $\lambda_\perp = 5$ nm in our calculation (see Appendix B). The small penetration depth is in direct contradiction with a theoretical calculation and certain experimental evidence thus far [20,21]. Recent measurements in muon spin rotation experiments have even shown penetration depths in the order of μm in bulk $NbSe_2$ [22]. However, our estimated value agrees with previous work done on similar junctions as the ones described in Refs. [16,17]. The discrepancy only exists when comparing transport results and other direct penetration depth measurements.

The exfoliated flakes used to build junction devices are typically smaller than the theoretically predicted $\lambda_\perp$. An effective penetration depth should be incorporated. However, our flakes are well within the bulk limit where the critical temperatures do not vary with sample thickness [23]. Therefore the bulk $\lambda_\perp$ should still be in effect. If an effective London penetration depth is to be taken into consideration, it does clarify the similar reduced values reported in other $NbSe_2$ based heterostructure Josephson junctions. However, further discussion about the origin of this inconsistency is beyond the scope of this paper.

V. CONCLUSION

To summarize, we have presented a simple model to understand the origin of the irregular superconducting critical

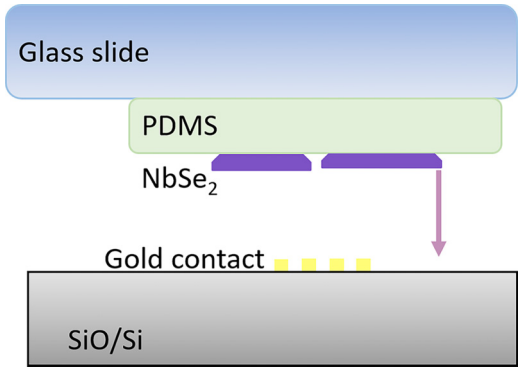

FIG. 6. A schematic of our device fabrication process. Two separate $NbSe_2$ flakes are stamped on top of gold contacts with a small overlapping area. A diffusive junction is fabricated when the stamping temperature is raised to be 180 °C whereas a clean junction is made at room temperature.

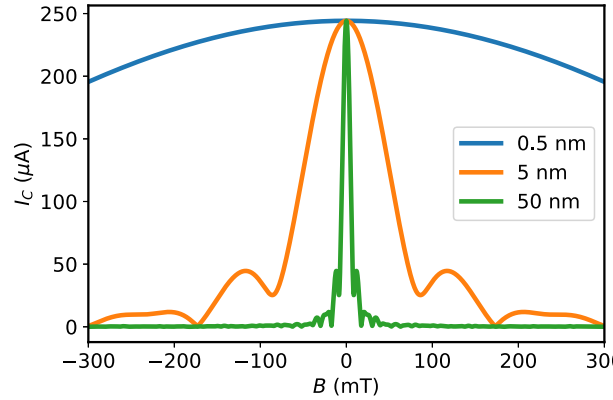

FIG. 7. The calculated critical current as a function of magnetic field strength at 35° with several different values of $\lambda_\perp$. Our measured data are closest to the curve with a penetration depth of 5 nm.

current magnetic interference patterns in heterostructure Josephson junctions. Using this model, we argue that these patterns are dictated by both the orientation of the magnetic field and the exact geometry of the interface between the $NbSe_2$ flakes. In almost all field directions, sidelobes are strongly suppressed, making it unlikely that one measures the ideal Fraunhofer pattern in such junctions. Moreover, for certain field directions, the pattern will appear Gaussian rather than Fraunhofer-like, even for clean junctions.

ACKNOWLEDGMENTS

This research was made possible by financial support from the Dutch Science Foundation NWO. The authors are grateful for fruitful scientific discussion with Remko Fermin, Kaveh Lahabi, Jiasen Niu, Federica Galli, and Jan Aarts, and technical support from Marcel Hesselberth and Douwe Scholma.

APPENDIX A: DEVICE FABRICATION

Our junctions are fabricated with the commercially available stamping stage by HQ graphene. See Fig. 6 for a schematic of our device fabrication process.

APPENDIX B: CRITICAL CURRENT OSCILLATION PATTERN WITH DIFFERENT *c*-AXIS PENETRATION DEPTHS

Figure 7 shows the critical current oscillation pattern for device C1 at 35° (corresponding to results in Fig. 5) with several different $\lambda_\perp$ values. Because we have assumed a homogeneous supercurrent density across the overlapping area, the width of the central peak is inversely proportional to $2\lambda_\perp$ in a linear fashion, as shown in the graph.

Our data support that $\lambda_\perp = 5$ nm at 1.5 K, and using a good approximation of $\lambda_\perp$ dependence of T [24], we find $\lambda_\perp(0\ \mathrm{K}) = 5$ nm.

[1] K. S. Novoselov, A. K. Geim, S. V. Morozov, D. Jiang, Y. Zhang, S. V. Dubonos, I. V. Grigorieva, and A. A. Firsov, Science **306**, 666 (2004).
[2] K. S. Novoselov, A. Mishchenko, A. Carvalho, and A. H. Castro Neto, Science **353**, aac9439 (2016).
[3] X. Xi, Z. Wang, W. Zhao, J.-H. Park, K. T. Law, H. Berger, L. Forró, J. Shan, and K. F. Mak, Nat. Phys. **12**, 139 (2016).
[4] E. Y. Andrei and A. H. MacDonald, Nat. Mater. **19**, 1265 (2020).
[5] A. K. Geim and I. V. Grigorieva, Nature (London) **499**, 419 (2013).
[6] Y. Liu, N. O. Weiss, X. Duan, H.-C. Cheng, Y. Huang, and X. Duan, Nat. Rev. Mater. **1**, 16042 (2016).
[7] S. Kezilebieke, M. N. Huda, V. Vaňo, M. Aapro, S. C. Ganguli, O. J. Silveira, S. Głodzik, A. S. Foster, T. Ojanen, and P. Liljeroth, Nature (London) **588**, 424 (2020).
[8] R. Frisenda, E. Navarro-Moratalla, P. Gant, D. Pérez De Lara, P. Jarillo-Herrero, R. V. Gorbachev, and A. Castellanos-Gomez, Chem. Soc. Rev. **47**, 53 (2018).
[9] F. Pizzocchero, L. Gammelgaard, B. S. Jessen, J. M. Caridad, J. H. Lei Wang, P. Bøggild, and T. J. Booth, Nat. Commun. **7**, 11894 (2016).
[10] K. Kim, A. DaSilva, S. Huang, B. Fallahazad, S. Larentis, T. Taniguchi, K. Watanabe, B. J. LeRoy, A. H. MacDonald, and E. Tutuc, Proc. Natl. Acad. Sci. USA **114**, 3364 (2017).
[11] P. J. Zomer, M. H. D. Guimarães, J. C. Brant, N. Tombros, and B. J. van Wees, Appl. Phys. Lett. **105**, 013101 (2014).
[12] S. Y. F. Zhao, N. Poccia, X. Cui, P. A. Volkov, H. Yoo, R. Engelke, Y. Ronen, R. Zhong, G. Gu, S. Plugge, T. Tummuru, M. Franz, J. H. Pixley, and P. Kim, arXiv:2108.13455.
[13] J. Lee, W. Lee, G.-Y. Kim, Y.-B. Choi, J. Park, S. Jang, G. Gu, S.-Y. Choi, G. Y. Cho, G.-H. Lee, and H.-J. Lee, Nano Lett. **21**, 104469 (2021).
[14] M. Kim, G.-H. Park, J. Lee, J. H. Lee, J. Park, H. Lee, G.-H. Lee, and H.-J. Lee, Nano Lett. **17**, 6125 (2017).
[15] H. Wu, Y. Wang, Y. Xu, P. K. Sivakumar, C. Pasco, U. Filippozzi, S. S. P. Parkin, Y.-J. Zeng, T. McQueen, and M. N. Ali, Nature (London) **604**, 653 (2022).

[16] N. Yabuki, R. Moriya, M. Arai, Y. Sata, S. Morikawa, S. Masubuchi, and T. Machida, Nat. Commun. **7**, 10616 (2016).
[17] L. S. Farrar, A. Nevill, Z. J. Lim, G. Balakrishnan, S. Dale, and S. J. Bending, Nano Lett. **21**, 6725 (2021).
[18] R. C. Dynes and T. A. Fulton, Phys. Rev. B **3**, 3015 (1971).
[19] A. Castellanos-Gomez, M. Buscema, R. Molenaar, V. Singh, L. Janssen, H. S. J. van der Zant, and G. A. Steele, 2D Mater. **1**, 011002 (2014).
[20] J. J. Finley and B. S. Deaver, Solid State Commun. **36**, 493 (1980).
[21] J. D. Fletcher, A. Carrington, P. Diener, P. Rodière, J. P. Brison, R. Prozorov, T. Olheiser, and R. W. Giannetta, Phys. Rev. Lett. **98**, 057003 (2007).
[22] F. O. von Rohr, J.-C. Orain, R. Khasanov, C. Witteveen, Z. Shermadini, A. Nikitin, J. Chang, A. R. Wieteska, A. N. Pasupathy, M. Z. Hasan, A. Amato, H. Luetkens, Y. J. Uemura, and Z. Guguchia, Sci. Adv. **5**, eaav8465 (2019).
[23] A. I. Gubin, K. S. Il'in, S. A. Vitusevich, M. Siegel, and N. Klein, Phys. Rev. B **72**, 064503 (2005).
[24] V. V. Schmidt, in *The Physics of Superconductors*, 1st ed., edited by P. Muller and A. V. Ustinov (Springer, Berlin, 1997), p. 25.